



## Molecular Crystals and Liquid Crystals Science and Technology. Section A. Molecular Crystals and Liquid Crystals

Publication details, including instructions for authors and  
subscription information:

<http://www.tandfonline.com/loi/gmcl19>

## Photophysical Studies of Organic Molecules Included Within Zeolites

V. Ramamurthy<sup>a</sup> & J. V. Caspar<sup>a</sup>

<sup>a</sup> Central Research and Development, Experimental Station, The Du  
Pont Company, Wilmington, DE, 19880-0328, USA

Version of record first published: 27 Oct 2006.

To cite this article: V. Ramamurthy & J. V. Caspar (1992): Photophysical Studies of Organic Molecules  
Included Within Zeolites, Molecular Crystals and Liquid Crystals Science and Technology. Section A.  
Molecular Crystals and Liquid Crystals, 211:1, 211-226

To link to this article: <http://dx.doi.org/10.1080/10587259208025822>

PLEASE SCROLL DOWN FOR ARTICLE

Full terms and conditions of use: <http://www.tandfonline.com/page/terms-and-conditions>

This article may be used for research, teaching, and private study purposes. Any  
substantial or systematic reproduction, redistribution, reselling, loan, sub-licensing,  
systematic supply, or distribution in any form to anyone is expressly forbidden.

The publisher does not give any warranty express or implied or make any representation  
that the contents will be complete or accurate or up to date. The accuracy of any  
instructions, formulae, and drug doses should be independently verified with primary  
sources. The publisher shall not be liable for any loss, actions, claims, proceedings,  
demand, or costs or damages whatsoever or howsoever caused arising directly or  
indirectly in connection with or arising out of the use of this material.

## PHOTOPHYSICAL STUDIES OF ORGANIC MOLECULES INCLUDED WITHIN ZEOLITES

V. RAMAMURTHY AND J. V. CASPAR  
 Central Research and Development,<sup>#</sup>  
 Experimental Station, The Du Pont Company,  
 Wilmington, DE 19880-0328, USA.

(Received August 7, 1991)

<sup>#</sup> Contribution Number 5942.

**Abstract** Results of photophysical studies of organic molecules included in zeolites are presented. Influence of cations through heavy atom effect and light atom effect on the photophysical properties of organic molecules is emphasized. Use of photophysical probes to understand the interior features of zeolites has been demonstrated.

**Keywords:** zeolite, photophysical, heavy atom effect, electric field of zeolite cage, pyrene, DMABN

### INTRODUCTION: STRUCTURE OF ZEOLITES

Zeolites are crystalline aluminosilicate materials with open framework structures.<sup>1</sup> The primary building blocks of the zeolites are the  $[\text{SiO}_4]^{4-}$  and  $[\text{AlO}_4]^{5-}$  tetrahedra (see Figure 1). These tetrahedra are linked by all their corners to form channels and cages or cavities of discrete size with no two aluminum atoms sharing the same oxygen.

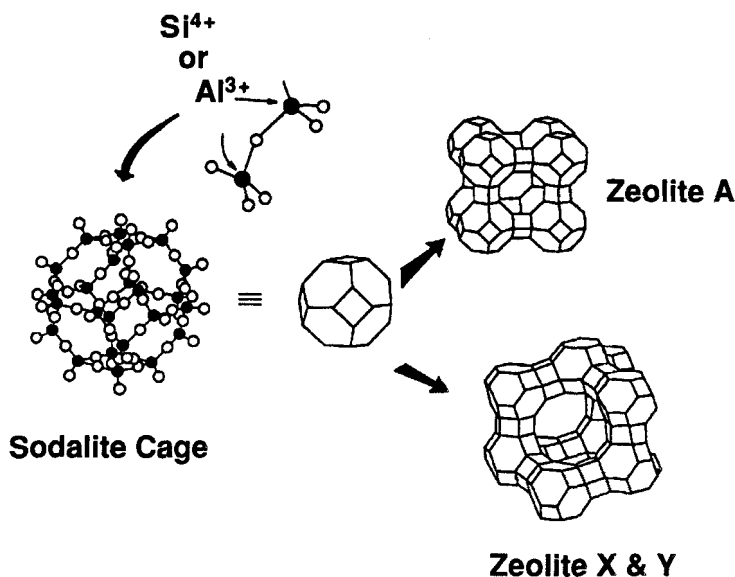


FIGURE 1. Illustrations of the  $[\text{SiO}_4]^{4-}$  and  $[\text{AlO}_4]^{5-}$  tetrahedra that are the primary building blocks of zeolites. Also shown are representations of the sodalite cage and zeolites A, X and Y.

As a result of the difference in charge between the  $[\text{SiO}_4]^{4-}$  and  $[\text{AlO}_4]^{5-}$  tetrahedra, the total framework charge of an aluminum-containing zeolite is negative and hence must be balanced by a cation, typically an alkali or alkaline earth metal cation. As such, zeolites can be represented by the empirical formula  $\text{M}_{2/n} \cdot \text{Al}_2\text{O}_3 \cdot x \text{SiO}_2 \cdot y \text{H}_2\text{O}$ , where M is the cation of valence  $n$  (typically Na, Ca, Mg, etc),  $x = 2-\infty$ , and  $y$  varies from 0 to approximately 10. These cations can generally be exchanged by conventional methods. The cations and water molecules present are located in the cages, cavities, and channels of the zeolites.

The numerous framework topologies of zeolites offer various systems of channels and cavities resulting in one-, two-, or three-dimensional diffusion for included guest molecules (Table 1). There are two types of structures: one provides an internal pore system comprised of interconnected cage structures; the second provides a system of uniform channels. Access to these channels, cages or cavities is through a pore or window which can be of the same size or smaller than the size of the channels, cages or cavities. It is the dimension of these pores which determines the size of molecules that can be adsorbed into these structures.

Among the various zeolites, faujasite type zeolites have attracted considerable attention. Since this paper is concerned only with faujasites no presentation on the structure of other zeolites will be made. The two synthetic forms of faujasite are referred to as zeolite X and Y and have the following typical unit cell composition:

X type  $\text{M}_{86}(\text{AlO}_2)_{86}(\text{SiO}_2)_{106} \cdot 264 \text{H}_2\text{O}$

Y type  $\text{M}_{56}(\text{AlO}_2)_{56}(\text{SiO}_2)_{136} \cdot 253 \text{H}_2\text{O}$

where M is a monovalent cation.

Charge-compensating cations present in the internal structure of zeolites are known to occupy three different positions in zeolites X and Y. As illustrated in Figure 2, the first type (site I), with 16 per unit cell (both X and Y), is located on the hexagonal prism faces between the sodalite units. The second type (site II), with 32 in number per unit cell (both X and Y), is located in the open hexagonal faces.

### CATION LOCATION INSIDE FAUJASITE CAGES

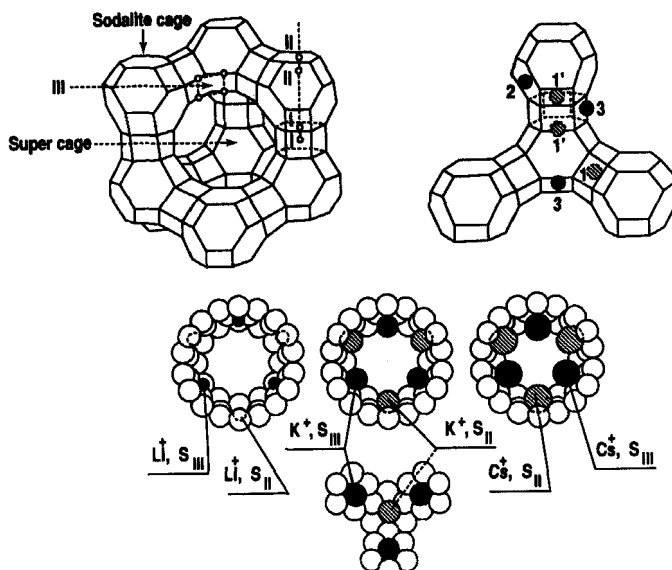


FIGURE 2. Supercage structure, cation location (I, II, III) within X and Y type zeolites. Bottom portion shows the reduction in available space (relative) within the supercage as the cation size increases.

The third type (site III), with 38 per unit cell in the case of X type and only eight per unit cell in the case of Y type, is located on the walls of the larger cavity. Only cations of sites II and III are expected to be readily accessible to the adsorbed organic. The free volume available for the organic within the supercage depends on the number and nature of the cation. The largest pore opening is a 12-ring with dimensions of about 7.4 Å. The supercages form a three-dimensional network with each supercage connected tetrahedrally to four other supercages through the 12-membered ring opening.

TABLE 1. Size of pore openings and dimensionality of the pore system for selected medium-pore and large pore molecular sieves. <sup>a</sup>

Molecular Sieve Name	Pore (window) Size (Å)	Channel/Cage Size
<i>Medium Pore Zeolites:</i>		
AlPO <sub>4</sub> -11	3.9 x 6.3	Single Channel
ZSM-23	4.5 x 5.2	"
Laumontite	4.0 x 5.3	"
Partheite	3.5 x 6.9	"
Theta-1	4.4 x 5.5	"
Dachiardite	3.4 x 5.3 and (3.7 x 4.8)	Two interconnected channels
Stilbite	4.9 x 6.1 and (2.7 x 5.6)	"
Epistilbite	3.4 x 5.6 and (3.7 x 5.2)	"
Ferrierite	4.2 x 5.4 and (3.5 x 4.8)	"
ZSM-11	5.3 x 5.4	"
ZSM-5	5.3 x 5.6 and 5.1 x 5.5	"
Eu-1	4.1 x 5.7	Channel with side pockets
Heulandite	3.0 x 7.6 and (3.0 x 7.6 and 3.3 x 4.6)	Three interconnected channels
<i>Large Pore Zeolites:</i>		
AlPO <sub>4</sub> -5	7.3	Single Channel
Cancrinite	5.9	"
ZSM-12	5.5 x 5.9	"
Linde Type L	7.1	Single channel with a lobe (d = 7.5)
Omega	7.4 (3.4 x 5.6)	Two noninterconnected channels
MAPSO-46	6.3 and (4.0)	Two interconnected channels
Gmelinite	7.0 and (3.6 x 3.9)	"
Mordenite	6.5 x 7.0 and (2.6 x 5.7)	"
Offretite	6.7 and (3.6 x 4.9)	"
Beta	7.5 x 5.7 and 6.5 x 5.6	Three dimensional channel
Faujasite (X and Y type)	7.4	Three dimensional channel with a cage (d = 12)
<i>Extra Large and Very Large Pore Zeolites:</i>		
AlPO <sub>4</sub> -8	7.9 x 8.7	Single Channel
VPI-5	12.1	"

<sup>a</sup> The numbers in paranthesis correspond to the smaller pore.

This paper is concerned with the photophysical behavior of organic molecules included in *faujasite* type of zeolites. Dependence of the physical characteristics of the cage on the cation (Li, Na, K, Rb, Cs and Tl) is highlighted. The physical properties of the cage that depend on the cation are the following (Table 2):

Electrostatic potential and electric field within the cage—depends on the charge density or electronegativity of the cation (light atom effect)

Mechanism available for singlet–triplet conversion— depends on the spin–orbit coupling parameter of the cation (heavy atom effect)

Vacant space available for the guest—depends on the size of the cation.

Information concerning the changes brought on the characteristics of the cage by the cation is gained by monitoring the photophysical properties of included organic molecules. The cation dependent variation of the vacant space available for the guest has been elegantly illustrated by Turro and his co-workers with the photorearrangement of dibenzylketone as an example.<sup>2</sup> Therefore, only the other two aspects listed above are the topic of discussion here.

TABLE 2. Dependence of Physical Parameters of M Y zeolites on the Cation<sup>a</sup>

Zeolite	Ionic Radius of the Cation (Å)	Electrostatic Field (V/Å) within the Cage	Electrostatic Potential (e/r)	Spin-Orbit Coupling of the Cation	Vacant Space within the Supercage(Å <sup>3</sup> )
LiY	0.6	2.1	1.67	—	834
NaY	0.95	1.3	1.05	27	827
KY	1.33	1.0	0.75	87	807
RbY	1.48	0.8	0.67	360	796
CsY	1.69	0.6	0.59	840	781

a. Ref. J. W. Ward, *J. Catalysis*, **1968**, *10*, 34.

## GUESTS WITHIN FAUJASITES

To be able to understand and predict the photobehavior of a guest molecule within zeolites one should know the exact location of the guest within these structures. Since all guest molecules exert some motion within the channels/cages/cavities of zeolites, x-ray structural characterization has not been possible. However, considerable literature exists on the characterization of the location of guest molecules within zeolites based on other techniques (uv, ir, nmr, neutron diffraction, small angle neutron scattering etc.).<sup>3</sup> Most of these studies are concerned with small molecules such as benzene, *p*-xylene, and pyridine, molecules not of primary concern to photochemists. These studies have shown that at high loadings there are three distinct types of benzene molecules, located within the supercages—one at the cation site (site II or III), one at the 12-ring window site, and the other corresponding to benzene clusters within the cage. At low loading levels the clustering can be avoided and the distribution between the window and the cation sites can be controlled by the loading level and by the nature of the cation. It has also become clear through extensive nmr investigations that the molecules are not stationary at these sites.<sup>4</sup> They undergo rotational motions at the site itself and also jump from one site to the other. We assume in this study that at low loading levels the included molecule reside within a cage, probably close to the cation. No extensive physical characterization of the guest within the zeolite has been made.

## LIQUID OR SOLID LIKE?

The luminescence spectra of the zeolite-included organic guests are generally similar to those in an organic solution or glass. This is evident when the fluorescence spectra of phenanthrene and chrysene are compared in the crystalline state, in methylcyclohexane glass (MCH) and in Na-X zeolite (Figure 3). A close similarity in fluorescence spectra between MCH glass and Na-X zeolite is obvious and this suggests that the aromatic molecules included in the cages of zeolites have a microenvironment that is very much like that in an organic solution and do not resemble that in the crystalline state. Thus the guest within a solid host is more liquid than solid like.

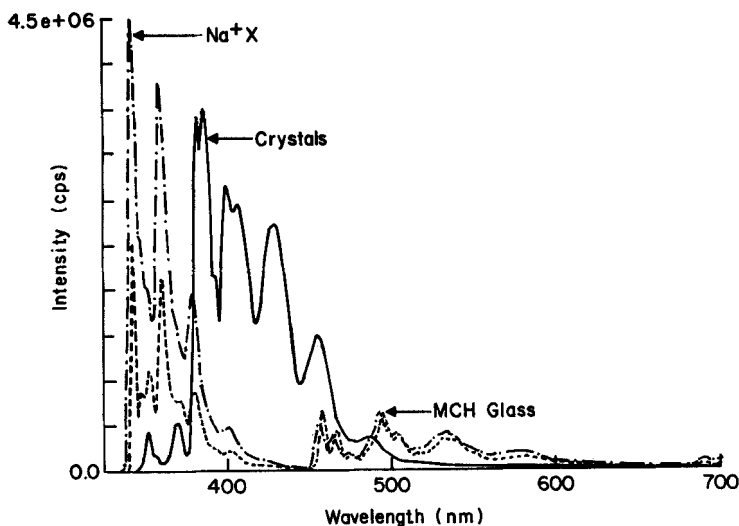


FIGURE 3. Fluorescence spectra of phenanthrene in various media. Notice the similarity between the MCH glass and zeolite included samples.

#### SITE INHOMOGENEITY AND MULTIPLE OCCUPANCY

The distribution of organic molecules within zeolites may or may not be uniform. This also means that the microenvironment around the guest molecules within a zeolite may not be uniform. Inhomogeneity in the microenvironment around a guest can arise for two reasons: variation in the occupancy number within a cage and the presence of sites of varying microenvironment. Even at low loading levels the cages may not be uniformly occupied, i.e., some may be singly occupied, some multiply occupied, while others not occupied at all. *The factors controlling the distribution pattern of guests within zeolites is an important problem yet to be addressed.*

Phosphorescence spectra of *trans*-stilbene included in Tl-X are shown in Figure 4. The emission maxima depend on the wavelength of excitation. This dependence is attributed to the presence of various rotational (phenyl ring rotated with respect to the double bond) conformers of *trans*-stilbene within the supercage (Chart 1).<sup>5</sup> This is unlike *trans*-stilbene dissolved in an organic solvent where a single minimum energy conformation is favored. Such a wavelength dependent phosphorescence is also seen with other olefins such as 1,2-dinaphthyl ethylene and 1,4-diphenylbutadiene. Thus all guest molecules included in zeolite cages should not be considered to be identical. Interconversion between isomers which may be fast in solution may not occur at all when they are adsorbed onto zeolite surface.

Emission from pyrene and pyrenealdehyde included in X zeolite are shown in Figures 5 and 6. Both monomer and excimer emissions are seen.<sup>6</sup> While in solution both monomer and excimer emissions have the same excitation spectra, in zeolite matrix the excitation spectra for the monomer and the excimer emissions differ. This implies that there are two types of pyrene molecules in the cages of faujasites. We believe that the difference arises from the fact that the guest molecules are not uniformly distributed within the cages: cages of both single and double occupancies are present. While monomer emission comes from molecules present in both types of cages, the excimeric emission originates from molecules present only in doubly occupied cages. The absorption spectra for the pyrene and pyrenealdehyde in these two environments probably differ slightly which is reflected in their excitation spectra.

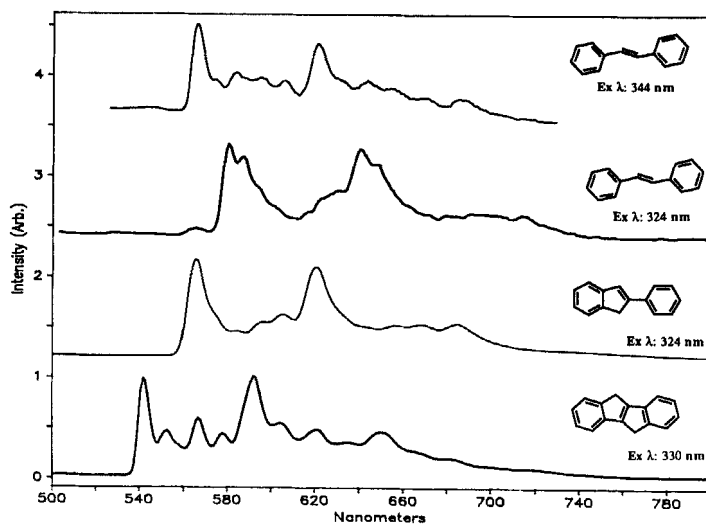


FIGURE 4. Phosphorescence spectra of *trans*-stilbene and related systems included in  $\text{Ti}^{+}$ -exchanged zeolites. Note that the emission maxima for *trans*-stilbene in TI-X depends on the excitation wavelength (324 and 344 nm).

### Phosphorescence $\lambda_{\text{max}}$

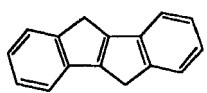
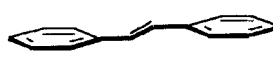
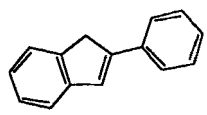
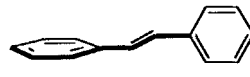
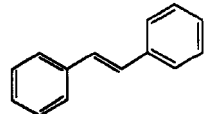
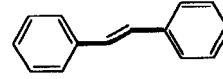
	548, 595, 652	
	567, 595, 680	
	580, 636, 698	

CHART 1. A comparison between phosphorescence emission maxima of various conformationally constrained *trans*-stilbenes. On the right side the restricted conformations of *trans*-stilbene are also shown.

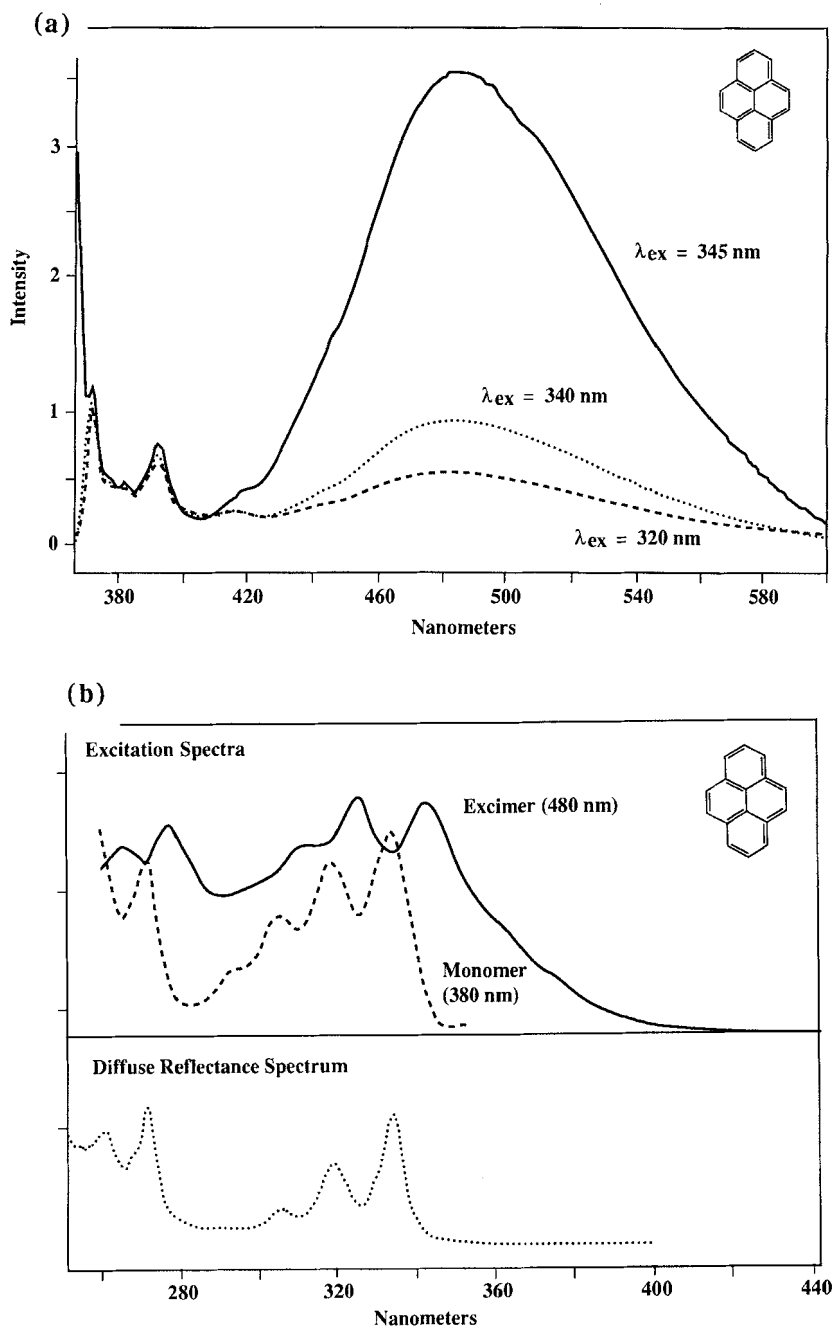


FIGURE 5. Emission (a) and excitation and diffuse reflectance (b) spectra of pyrene within Rb Y zeolite. Note the following: excitation spectra of the monomer and excimer differ; correspondence between the excitation spectra of the monomer and diffuse reflectance spectrum is excellent and the monomer to excimer emission ratio vary with the wavelength of excitation.



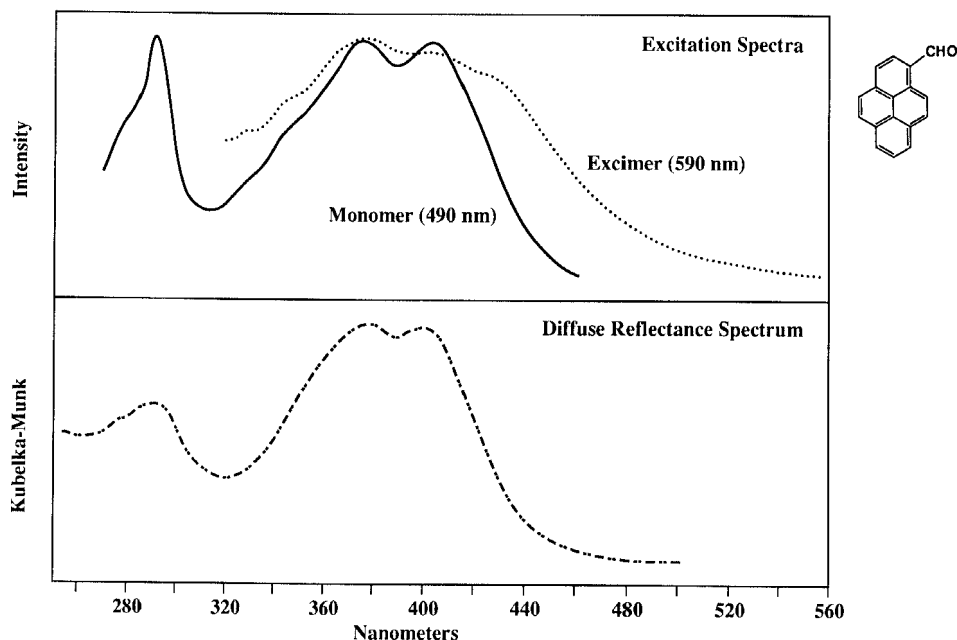


FIGURE 6. Excitation and diffuse reflectance spectra of pyrenealdehyde within Li X zeolite. Note the following: excitation spectra of the monomer and excimer differ and correspondence between the excitation spectra of the monomer and diffuse reflectance spectrum is excellent.

We have also observed multiexponential decay for naphthalene triplets in M-X (M = K, Rb, and Cs) zeolites.<sup>7</sup> Interestingly at temperatures below 150 K the decay is single exponential. However, at higher temperatures the lifetime is determined by at least two independent first-order decays (Figure 7).

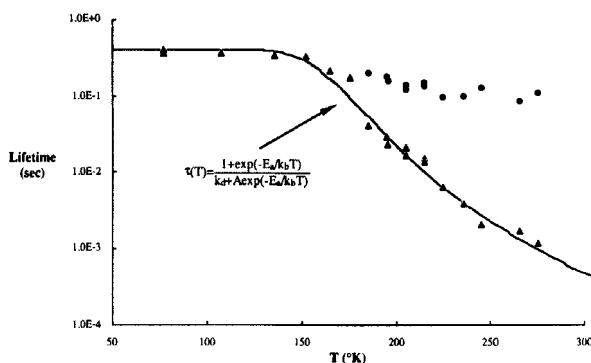


FIGURE 7. Temperature dependent decay of triplet naphthalene included in Cs-X. Note single exponential decay at temperatures below 150 K and double exponential decay above 150 K.

This suggested the presence of at least two independent sites for naphthalene in M-X zeolites. Consistent with this conclusion time-resolved emission spectra of naphthalene in Cs-X differ slightly for the slow and long-decaying components.

The above studies conclusively demonstrate that there is a wide range of possible sites or environments for guest molecules within the zeolite interior. The system is best described as "microheterogeneous".

#### VARIATION IN SPIN-ORBIT COUPLING PARAMETER: HEAVY-ATOM (CATION) EFFECT

In this section we illustrate how the change in cation alters the effective spin-orbit coupling available for a guest molecule within a cage. Such changes offer an unique opportunity to control the concentrations of the singlet and the triplet excited states of guest molecules. As seen in Table 2, the spin-orbit coupling parameter is directly related to the mass of the cation. We have been able to observe phosphorescence for systems for which previous attempts to record phosphorescence have yielded only negative results, by including them in  $\text{Tl}^+$  exchanged zeolites.

As shown in Figure 8, the emission spectrum of naphthalene is profoundly affected by inclusion in faujasites. For low-mass cations such as  $\text{Li}^+$  and  $\text{Na}^+$ , the emission spectra show the typical naphthalene blue fluorescence.<sup>8</sup> However, as the mass of the cation increases (e.g., from  $\text{Rb}^+$  to  $\text{Cs}^+$  to  $\text{Tl}^+$ ), there is a dramatic decrease in fluorescence intensity and a simultaneous appearance of a new vibronically structured low-energy emission band that is readily identified as the phosphorescence of naphthalene. This effect is found to be general.

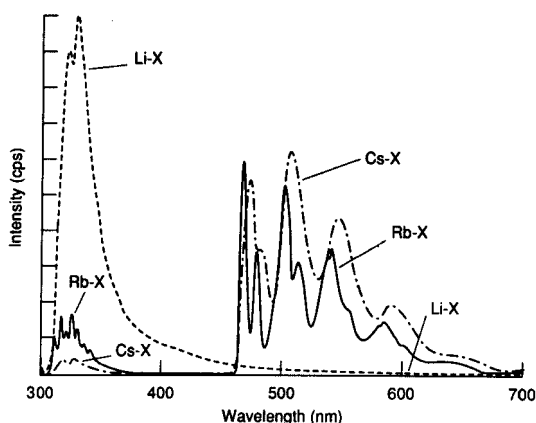


FIGURE 8. Emission spectra of naphthalene included in various cation-exchanged X zeolites. Note the ratio of fluorescence to phosphorescence emission depends on the cation.

Intense phosphorescence *alone* is observed for a wide range of different organic guests such as anthracene, acenaphthene, phenanthrene, chrysene, fluoranthene, pyrene, and 1,2,3,6,7,8-hexahydropyrene when included in  $\text{Tl}^+$ -exchanged faujasites. The only set of examples of guests for which phosphorescence is not observed are fused aromatics, which are too large in diameter to fit through the 8 Å windows of the X- and Y-type zeolites (e.g., coronene and triphenylene). In these cases the observed emission spectrum closely resembles that for the crystalline guest with no evidence of heavy-atom perturbation.

The correlation of the appearance of the phosphorescence with cation mass clearly suggests that the effect is due to an external heavy-atom perturbation. It is well known that the effect of external heavy-atom perturbation scales with the square of the perturbers spin-orbit coupling constant,  $\xi^2$  and that a log-log plot of  $\tau^{-1}$  vs.  $\xi^2$  should be linear with a maximum predicted slope of unity.<sup>7</sup> As shown in Figure 9, the expected dependence is observed. The magnitude of the heavy-atom effect observed in

zeolites is significantly larger than that observed for the 1,5-naphtho-22-crown-6 exchanged with heavy-atom cations where the cation is rigidly held over the naphthalene  $\pi$  face.

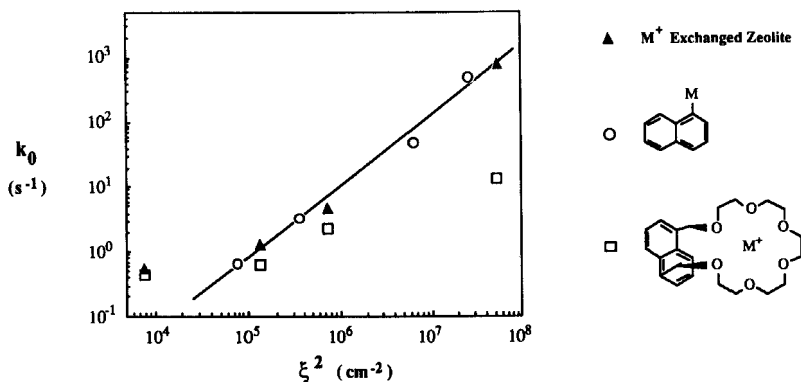
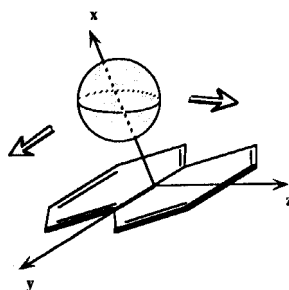


FIGURE 9. Correlation between the triplet decay and the spin-orbit parameter: for naphthalene included in cation exchanged zeolites. For comparison, results on other related systems are also shown.

In fact, the zeolite samples show heavy-atom effects nearly as large as for a series of 1-halonaphthalenes where the perturbers are covalently attached to the chromophore. The unusually high external heavy-atom effect observed here is attributed both to the close approach between naphthalene and the heavy atom (cation), which is enforced by the zeolite supercage, and to the presence of more than one heavy atom (cation) per supercage, which leads to high effective concentrations of the heavy atom in the vicinity of the naphthalene. In order to obtain a picture of the geometry of the cation-chromophore complexes in X- and Y-type faujasites, we took advantage of the heavy-atom-induced phosphorescence, which allows the use of optical detection of magnetic resonance (ODMR) in zero applied magnetic field. The sublevel specific dynamics for adsorbed naphthalene show a distinct increase in relative radiative character and in total rate constant of decay of the out-of-plane x-sublevel with increasing mass of the cation perturber.<sup>9</sup> Interpretation of the kinetic results on the basis of a well-established model suggests that the naphthalene is adsorbed through its  $\pi$  cloud at a cation site as shown below.



It is easy to appreciate the potential of the unusual environment of zeolites when one realizes that even olefins, systems that under normal conditions do not show phosphorescence, emit from their triplet states when included in  $\text{Tl}^+$ -exchanged zeolites.<sup>5</sup> Excitation of *trans*-stilbene included in  $\text{Tl}^+$ -

exchanged faujasites (X and Y type) and pentasils (ZSM-5, -8, and -11) emits intense phosphorescence both at room temperature and at 77 K (Figure 4). Emission in the 550–750 nm region having a sub-msec lifetime is quenched by oxygen. Furthermore, the emission band positions are in the same region reported earlier for phosphorescence (EPA glass  $\lambda_{\text{max}}$ : 580, 636, and 698 nm). More importantly, the excitation spectra consist of both  $S_0$  to  $S_1$  and  $S_0$  to  $T_1$  transitions, the latter being in the same region recorded by the oxygen perturbation technique (Figure 10).

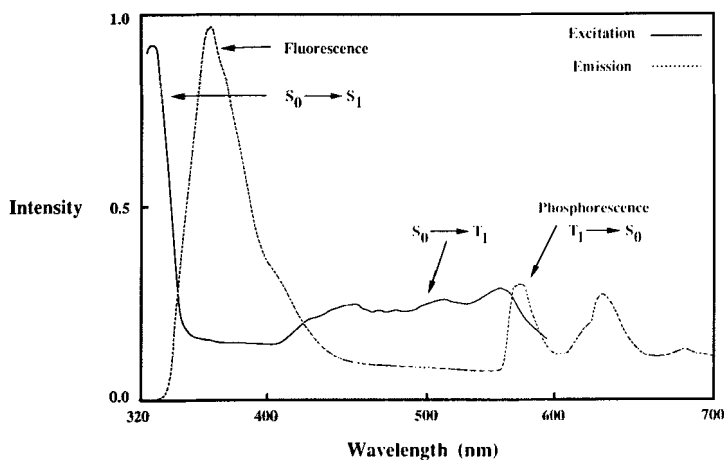


FIGURE 10. Phosphorescence emission and excitation spectra of *trans*-stilbene in Tl-X. Excitation monitored at 627 nm.

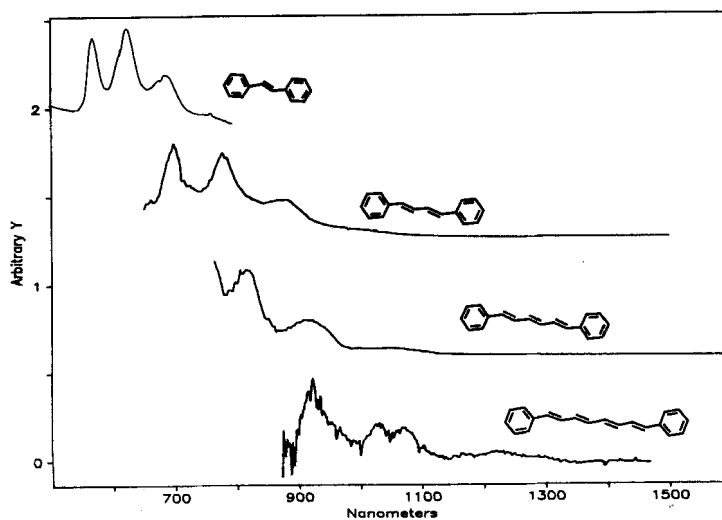


FIGURE 11. Phosphorescence spectra of several  $\alpha,\omega$ -diphenyl polyenes included in  $\text{Tl}^+$ -exchanged zeolites.

In an effort to expand the utility of these zeolite hosts for the observation of phosphorescence from triplet states that have not heretofore been observable, we have investigated the spectroscopy of the *all-trans*- $\alpha,\omega$ -diphenylpolyenes 1,4-diphenyl-1,3-butadiene (DPBD), 1,6-diphenyl-1,3,5-hexatriene (DPHT), and 1,8-diphenyl-1,3,5,7-octatetraene (DPOT) included in heavy-atom-exchanged zeolites.<sup>9</sup> Figure 11 shows the observed phosphorescence of the  $\alpha,\omega$ -diphenylpolyenes included in  $\text{Ti}^{+}$ -exchanged X-type faujasite. At 77 K, a well-resolved structured emission for each of the polyenes with a prominent vibronic spacing of 1200–1400  $\text{cm}^{-1}$  as expected for triplet phosphorescence was observed. The singlet–triplet energy gaps ( $\Delta T_1 \rightarrow S_0$ ) obtained from the observed zero–zero lines are in excellent agreement with literature predictions from  $S_0 \rightarrow T_1$  absorption spectra obtained by the  $\text{O}_2$  perturbation method and from energy-transfer studies. These results demonstrate the utility of zeolite hosts as spectroscopic matrices for the investigation of organic triplet states.

#### VARIATION OF CHARGE DENSITY AND ELECTRIC FIELD WITHIN THE CAGE: LIGHT–ATOM (CATION) EFFECT

As shown in Table 2 the charge density, electrostatic field and electrostatic potential of the cation vary with its size. While the charge density depends only on the size of the cation, the electric field within a cage is expected to depend both on the size and on the number of cations. In this section both aspects (charge density and electric field) are discussed.

Based on the  $^2\text{H}$  nmr of phenanthrene in  $\text{M}^{+}$  X zeolites we have been able to show that the strength of binding interaction between the cation and the guest molecule is directly dependent on the charge density/electrostatic potential of the cation.<sup>10</sup> The higher the charge density (i.e., charge per unit volume of the cation), the stronger the binding ( $\Delta H$  binding:  $\text{Na}^{+}$ , 14.9;  $\text{K}^{+}$ , 11.0;  $\text{Cs}^{+}$ , 7.9 kcal  $\text{mole}^{-1}$ ). If such electronic interactions also influence the photophysical properties of the guest, the light cations are expected to have more influence than the heavier and the larger ones—thus the name "light atom effect."

Pyrene, pyrenealdehyde and *para*-dimethylaminobenzonitrile have been used as polarity probes for various microheterogeneous systems.<sup>11</sup> Polarity within a cage of X and Y zeolite does not have the same meaning as in solution. Within the cage there is electric field due to the charged cations. Micropolarity of the medium is in a way reflection of the electric field provided by cations. Therefore, polarity within a cage has only a loose meaning. While the phenomenon monitored and the mechanism responsible for the change is different in each one of the probes mentioned above, they are capable of reporting, at least in a qualitative manner, the micropolarity of the cage. In the case of pyrene one monitors the intensity of the various vibronic bands of the singlet emission (Ham effect). We have measured the ratio of the band 5 (~392 nm) to band 1 (~371 nm) ( $I_5/I_1$ ) (Figure 12). In the case of pyrenealdehyde the monomer fluorescence maximum depends on the polarity (Figure 13). *para*-Dimethylaminobenzonitrile gives rise to a new emission from the twisted state in a polar medium (Figure 14). The emission from the twisted state depends on the polarity. We have used all three molecules as polarity probes and the results are summarized in Table 3.<sup>12</sup>

It is clear from Table 3 that as per pyrenealdehyde and *para*-dimethylaminobenzonitrile the cage is more polar or possess high electric field when the cation is Li or Na. Also the polarity/electric field of the cage decreases with the cation size ( $\text{Li} > \text{Na} > \text{K} > \text{Rb} > \text{Cs}$ ). Furthermore, the cage is more polar in the case of X zeolites than in Y zeolites. This is due to the difference in the number of cations in these two zeolites. The results on pyrene are generally consistent with those on the other two probes. However, pyrene is unable to sense the difference between Li, Na and other cations. This we believe is due to the difference in location of the probes. While both pyrenealdehyde and *para*-dimethylaminobenzonitrile are expected to be close to the cation due to their strong binding interaction with it, pyrene because of its size may not be able to reach the cation site. Especially, Li and Na which are expected to be buried within the oxygen windows of the cage may not be accessible to pyrene. Pyrene's effectiveness as a probe is obvious when one notices that it is able to see the difference in the polarity of a cage between K, Rb and Cs as cations and that between X and Y zeolites. Based on the above three probes, one can conclude that the zeolite cages are very polar and the micropolarity varies with the cation.

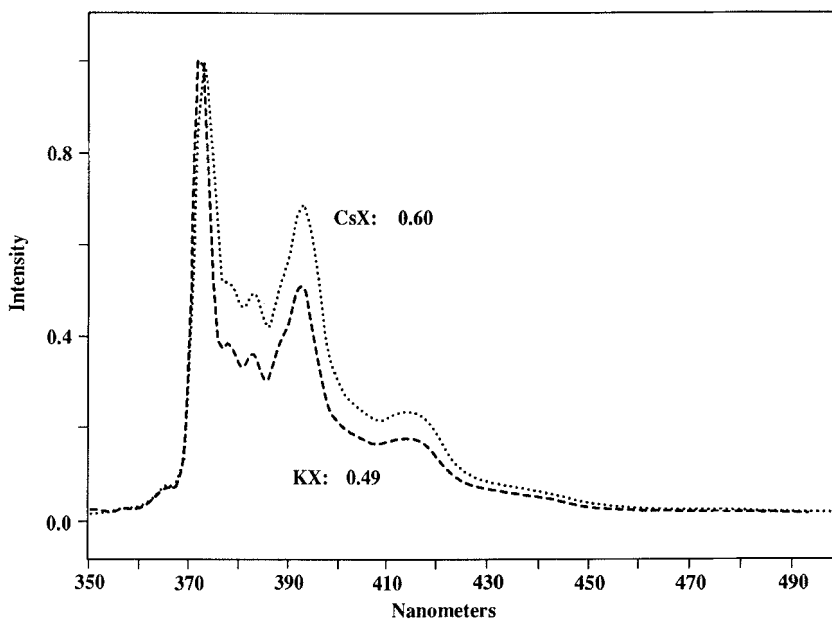


FIGURE 12. Fluorescence emission spectra of pyrene in Cs X and K X zeolites. Notice the change in the intensities of the vibronic band at 392 and 371 nm.

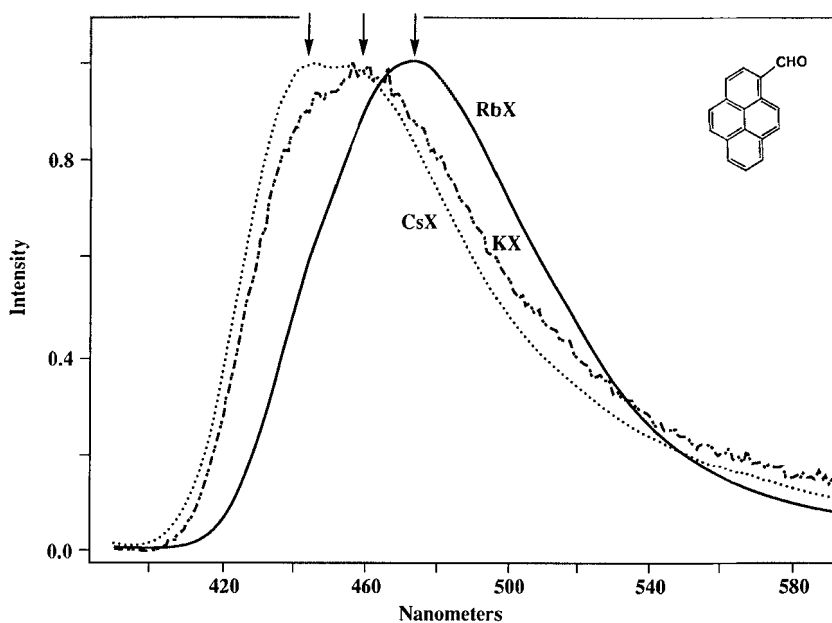


FIGURE 13. Fluorescence emission spectra of pyrenealdehyde in Na X, K X and Cs X zeolites. Notice the fluorescence maximum shift with respect to the cation.

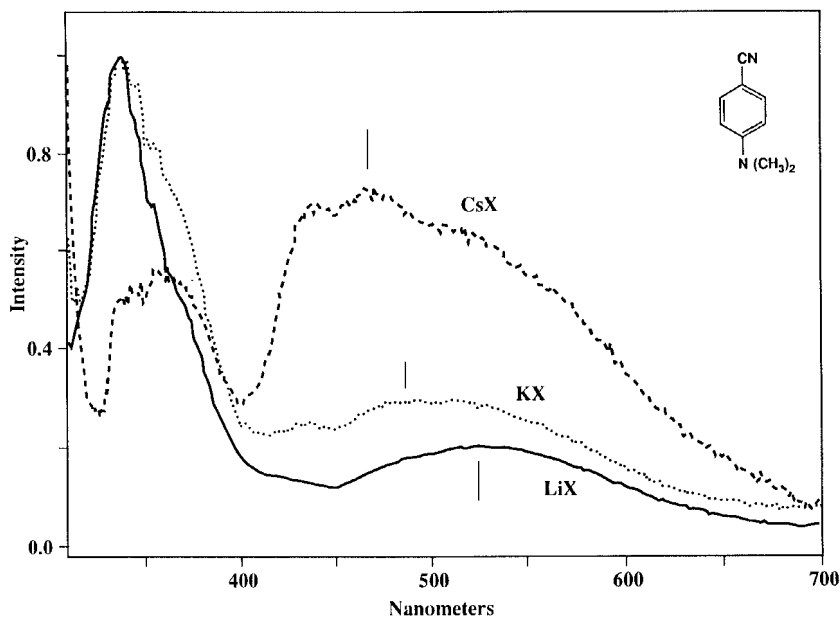


FIGURE 14. Fluorescence emission spectra of 4-dimethylaminobenzonitrile in Li X, K X and Cs X zeolites. Notice the shift in TICT emission maximum with respect to the cation.

TABLE 3: Micropolarity of zeolite cages as probed by three conventional photochemical probes

Zeolite	Pyrene <sup>a</sup> I <sub>5</sub> /I <sub>1</sub>	DMABN <sup>b</sup> emission $\lambda_{\max}$	Pyrenealdehyde <sup>c</sup> emission $\lambda_{\max}$
LiX	0.58	337 and 535 nm	481 nm
NaX	0.60	338 and 528	473
KX	0.49	336 and 510	460
RbX	0.53	339 and 477	454
CsX	0.60	342 and 471	450
LiY	0.81	334 and 523	467
NaY	0.73	334 and 512	463
KY	0.56	335 and 500	450
RbY	0.60	335 and 463	443
CsY	0.71	335 and 440 <sup>d</sup>	440
Cyclohexane	1.39	340 only	392
Acetonitrile	0.78	337 and 485	415
Water	–	347 and 553	480

a. Intensity of the monomer fluorescence at 392 nm vs 372 nm.

b.  $\lambda_{\max}$  of the normal emission and emission from TICT state.

c.  $\lambda_{\max}$  of the monomer emission.

d. emission corresponds to phosphorescence.

We have also observed that the lifetimes of the excited singlet and triplet states of guests are influenced by the cations. A consistently shorter lifetime was recorded in Li-X than in Na-X for the excited singlet state of aromatic molecules (Table 4).<sup>13</sup> A similar cation-dependent variation in the triplet lifetime of valerophenone has been recorded by us<sup>14</sup> (Li-X, 4; Na-X, 0.4; and K-X, 0.9  $\mu$ s). All these are tentatively attributed to the cation interaction with the guest.

TABLE 4. A comparison of the singlet lifetimes (nanosec) of aromatics in various cation exchanged zeolites

Zeolite	Naphthalene	Acenaphthene	Phenanthrene	Pyrene	Chrysene
LiX	32.6	5.0	29.8	92.4	19.2
NaX	49.1	11.6	36.6	115.4	27.1
KX	19.4	13.1	27.8	161.4	39.2

## SUMMARY

It is clear from this presentation that photophysical probes can provide useful information regarding the microenvironment of the zeolite cage. Such knowledge can be useful to predict the photochemical behavior of included guest molecules.<sup>15</sup>

## ACKNOWLEDGEMENT

It is a pleasure to thank Drs. D. R. Corbin and D. F. Eaton for their valuable contribution to the success of this work. Technical assistance by D. Sanderson and A. Pittman and P. Hollins has made this work possible.

## REFERENCES

1. R. M. Barrer in *Inclusion Compounds I*, J. L. Atwood, J. E. D. Davies, and D. D. MacNicol, eds., 1984, Academic Press: London, pp. 191-248.  
W. M. Meier and D. H. Olson in *Atlas of Zeolite Structure Types*, Butterworths: Cambridge, 1987 (Second Revised Edition).  
D. W. Breck, *Zeolite Molecular Sieves: Structure, Chemistry, and Use*, John Wiley and Sons, New York, 1974.  
A. Dyer, *An Introduction to Zeolite Molecular Sieves*, John Wiley and Sons, Bath, 1988.  
H. van Bekkum, E. M. Flanigen and J. C. Jansen, eds., *Introduction to Zeolite Science and Practice*, Elsevier, Amsterdam, 1991.  
R. Szostak, *Molecular Sieves. Principles of Synthesis and Identification*, Van Nostrand, New York, 1989.
2. N. J. Turro and P. Wan, *J. Am. Chem. Soc.*, **1985**, *107*, 678.  
N. J. Turro, *Pure Appl. Chem.*, **1986**, *58*, 1219.  
N. J. Turro in *Molecular Dynamics in Restricted Geometries*, J. Klafter and J. M. Drake, eds., 1989, John Wiley, New York, p. 387.
3. For a few recent references:  
A. de Mallman and D. Barthomeuf, *Zeolites*, **1988**, *8*, 292.  
A. de Mallman and D. Barthomeuf, *J. Chem. Soc. Chem. Commun.*, **1989**, 129.  
A. de Mallman, S. Dzwigaj and D. Barthomeuf in *Zeolites: Facts, Figures, Future*, P. A. Jacobs and R. A. van Santen, eds., 1989, Elsevier, Amsterdam, 935.



- P. J. O'Malley, *Chem. Phys. Lett.*, **1990**, *166*, 340.  
 R. Ryoo, S. B. Liu, L. C. de Menorval, K. Takegoshi, B. Chmelka, M. Trecoske and A. Pines, *J. Phys. Chem.*, **1987**, *91*, 6575.  
 L. C. de Menorval, D. Raftery, S. B. Liu, K. Takegoshi, R. Ryoo and A. Pines, *J. Phys. Chem.*, **1990**, *94*, 27.  
 A. N. Fitch, H. Jobic and A. Renouprez, *J. Chem. Soc., Chem. Commun.*, **1985**, 284.  
 A. N. Fitch, H. Jobic and A. Renouprez, *J. Phys. Chem.*, **1986**, *90*, 1311.  
 M. Czjek, T. Vogt and H. Fuess, *Angew. Chem. Int. Ed. Engl.*, **1989**, *28*, 770.  
 H. Jobic, A. Renouprez, A. N. Fitch and H. J. Lauter, *J. Chem. Soc., Faraday Trans. I*, **1987**, *83*, 3199.  
 A. de Mallmann and D. Barthomeuf, *J. Phys. Chem.*, **1989**, *93*, 5636.
4. For a few selected papers:  
 M. D. Sefcik, *J. Am. Chem. Soc.*, **1979**, *101*, 2164.  
 W. D. Hoffmann, *Z. Phys. Chemie, Leipzig*, **1976**, *257*, 315.  
 H. Lechert, W. Haupt and K. P. Wittern, *J. Catalysis*, **1976**, *43*, 356.  
 H. Lechert and H. J. Hennig, *Z. Naturforsch.*, **1974**, *29 A*, 1065.  
 M. Nagel, D. Michel and D. Geschke, *J. Colloid. Interfac. Sci.*, **1971**, *36*, 254.  
 J. B. Nagy, E. G. Deroune, H. A. Resing and G. R. Miller, *J. Phys. Chem.*, **1983**, *87*, 833.
  5. V. Ramamurthy, J. V. Caspar and D. R. Corbin, *Tetrahedron Letters*, **1990**, *31*, 1097.
  6. V. Ramamurthy and D. R. Sanderson, Unpublished results. Also see K. K. Iu and J. K. Thomas, *Langmuir*, **1990**, *6*, 471.
  7. J. V. Caspar, V. Ramamurthy and D. R. Corbin, *Coordination Chem. Rev.*, **1990**, *97*, 225.
  8. V. Ramamurthy, J. V. Caspar, D. R. Corbin and D. F. Eaton, *J. Photochem. Photobiol., A: Chemistry*, **1989**, *50*, 157.
  9. V. Ramamurthy, J. V. Caspar, D. R. Corbin, B. D. Schlyer and A. H. Maki, *J. Phys. Chem.*, **1990**, *94*, 3391.
  10. M. Hepp, V. Ramamurthy, D. Corbin and C. Dybowski, *J. Phys. Chem.* Submitted.
  11. K. Kalyanasundaram in *Photochemistry in Organized and Constrained Media*, V. Ramamurthy, ed., VCH Publishers, New York, 1991, p. 39.
  12. V. Ramamurthy, D. R. Sanderson and D. F. Eaton, Unpublished results.
  13. V. Ramamurthy, J. V. Caspar and D. F. Eaton, Unpublished results.
  14. V. Ramamurthy and L. Johnston, Unpublished results.
  15. For a summary see: V. Ramamurthy in *Photochemistry in Organized and Constrained Media*, V. Ramamurthy, ed., VCH Publishers, New York, 1991, p. 429.